Journal of Colloid and Interface Science **219,** 212–215 (1999)
Article ID jcis.1999.6473, available online at http://www.idealibrary.com on IDEAL®

NOTE

Study of the Dissolution of the Barium Sulfate (001) Surface with Hydrochloric Acid by Atomic Force Microscopy

Noncontact atomic force microscopy (NC-AFM) has been used to investigate the morphological changes of a freshly cleaved (001) surface of barium sulfate (barite) etched with an aqueous solution of 0.1 M HCl at room temperature. Shallow triangular etch pits with a height of 3.6 Å were developed in atomically flat (001) terraces. The etching of the surface was found to proceed in a layer-by-layer dissolution process. Because the crystal structure of barite exhibits a two-fold screw axis parallel to the *c* axis, "alternating" etch pits were formed, with any two consecutive etch pits pointing opposite to each other. These etch pits became deeper and more elongated along the *b* axis with time.

Key Words: **atomic force microscopy; barium sulfate; HCl; etch pit; dissolution.**

INTRODUCTION

Formation of mineral scale deposits is almost inevitable in industrial water, oil, and gas production systems. There are many scales that can be removed by chemical methods, and the chemicals used depend on the specific nature of the scale. Calcium carbonate, iron carbonate, iron sulfide, and iron oxide, for instance, are soluble in acids such as hydrochloric acid (1). Of all the common water-formed scale deposits, barium sulfate (barite) scale is the most troublesome because it is extremely insoluble ($K_{sp} = 10^{-9.99}$ at 25°C) in water (2), and cannot be removed by acid treatment (1). To dissolve barium sulfate scale, strong chelating agents must be used as so-called scale dissolvers, e.g., diethylenetriaminepentaacetic acid (DTPA) and ethylenediaminetetraacetic acid (EDTA) (3). The changes of barite (001) surfaces immersed in these solutions have been investigated by several investigators (4–7) using scanning force microscopy (SFM), which is also known as atomic force microscopy (AFM).

SFM has been shown to be a powerful technique for investigating morphological changes during mineral growth, precipitation, and dissolu-

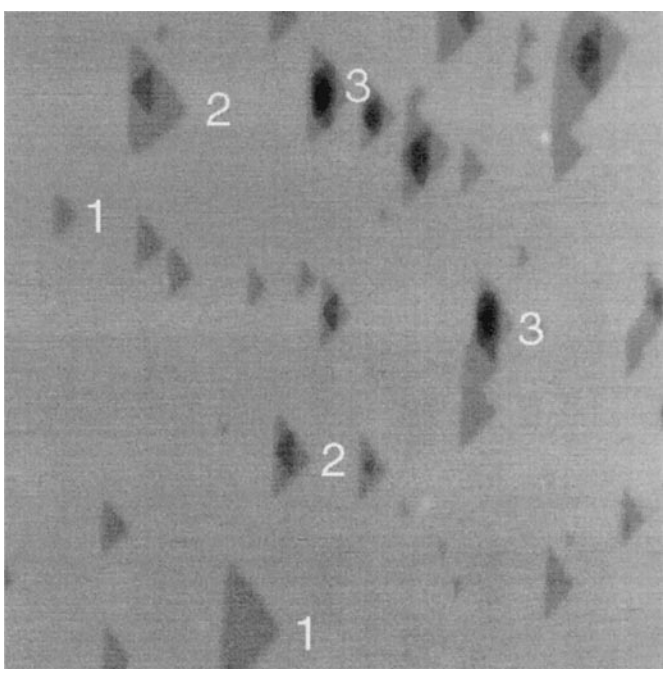

FIG. 1. NC-AFM image of a barium sulfate (001) surface treated with 0.1 M HCl at 20°C after 5 min. (1) Triangular etch pits with a depth of one-half of the unit cell. (2) Triangular etch pits with a depth of one unit cell dimension. These pits are characterized by a bottom with a triangular feature with an orientation opposite to the top of the etch pit. (3) Deeper etch pits that have a depth of more than one unit cell. Image size: 1 μm × 1 μm. Depth scale from black to white: 2.5 nm.

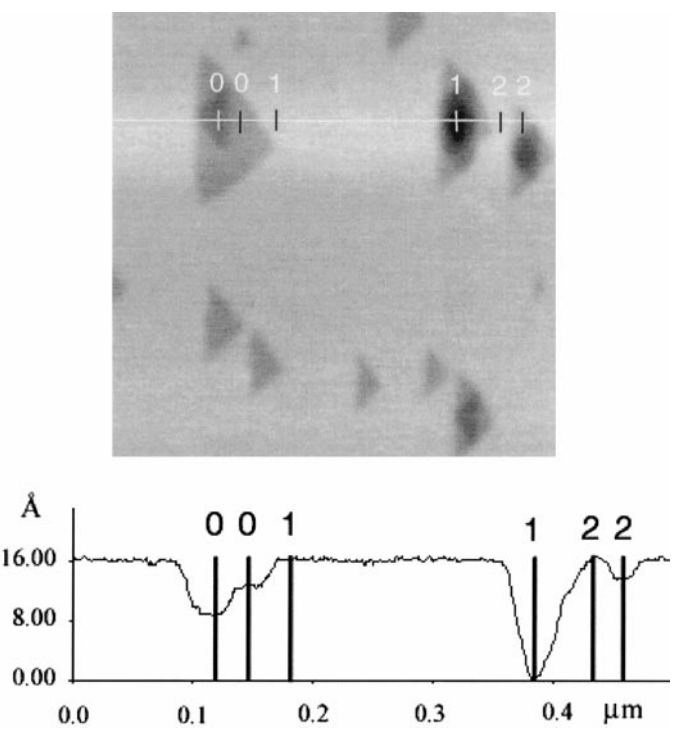

FIG. 2. Higher-magnification image of a region displayed in Fig. 1 and corresponding line profile along the *a* axis through three pits observed after immersion of the barite (001) surface in 0.1 M HCl for 5 min. The depths of the etch pits "0–0," "0–1," "1–1," and "2–2" are 3.64, 3.38, 16, and 3.46 Å, respectively. Image size: 0.5 μm × 0.5 μm. Depth scale from black to white: 2 nm.

0021-9797/99 $30.00

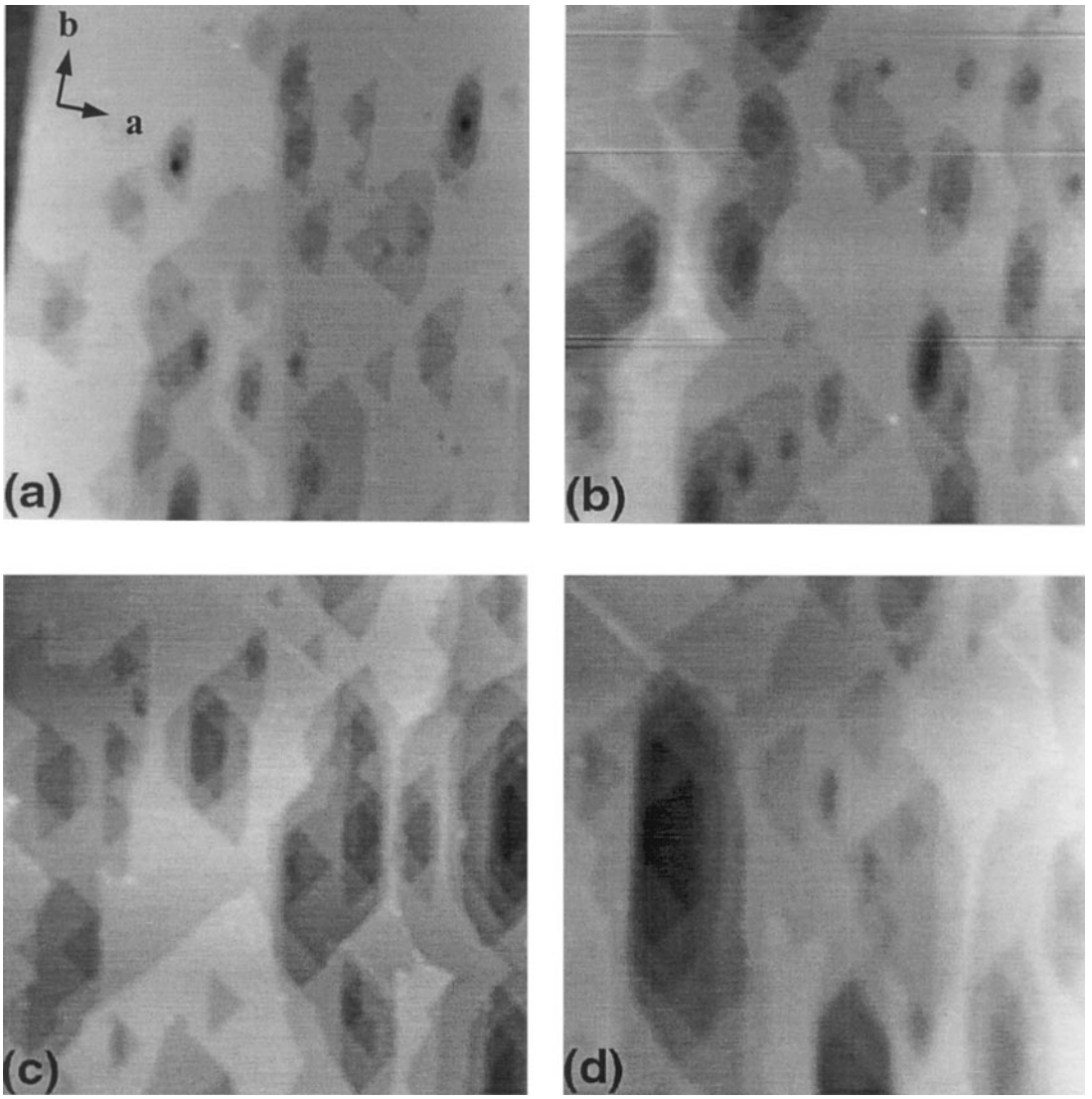

FIG. 3. NC-AFM images of a barium sulfate (001) surface after immersion in 0.1 M HCl at 20°C after (a) 15 min, (b) 25 min, (c) 40 min, and (d) 60 min. Image size: 2 μm $\times$ 2 μm. Depth scale from black to white: (a–c) 5 nm, (d) 6 nm.

tion (4–10). This technique allows direct observation of mineral surfaces in air, solution, or vacuum. *In situ* observations of reaction processes in real time at the mineral–solution interface with contact-mode AFM (CM-AFM) have provided valuable access to surface processes in the absence of undesirable artifacts caused by ambient exposures. However, when CM-AFM is used under liquids the results are sometimes affected by the measurement process, which can stimulate the dissolution process. Although contact forces are generally small in CM-AFM, the sample experiences both compressive forces originating from the tip/sample contact and shear forces attributed to the lateral scan movement. These effects often introduce artifacts (11).

In these studies, an improvement was achieved by using *ex situ* analysis by noncontact-mode AFM (NC-AFM), where the cantilever is driven at (or near) its resonant frequency with the tip oscillating at a few nanometers above the sample surface. Changes in the vibration amplitude reveal the topography of the sample (12). Since the tip is not in permanent contact with the sample surface, damage to the surface and/or surface modification caused by tearing and lateral shear forces (13) can be excluded.

In this Note, we present for the first time AFM images of the dissolution of the barite (001) surface in hydrochloric acid. HCl-induced dissolution of the barite (001) surface is interesting for two reasons: (i) analysis of these images provides new and complementary information on the reactivity of barite (001) surfaces, and (ii) rationalizing how mineral scales react and dissolve under chemical treatments. This will allow for the development of new, more efficient scale dissolvers. Such improvements are very important to the oil and gas industry.

EXPERIMENTAL METHODS

We used natural barite crystals (clear and colorless) from the Barrick Meikle Mine in Nevada. The bulk composition of those samples was $Ba_{0.91}Sr_{0.09}SO_4$, as analyzed by X-ray fluorescence spectroscopy. Sulfate scales are commonly found to contain a mixture of barium and strontium. Barite has an orthorhombic (space group P_{nma}) crystal structure with lattice parameters $a = 8.884$ Å, $b = 5.457$ Å, $c = 7.157$ Å, and $Z = 4$ (14). Each unit cell has two $BaSO_4$ layers parallel to (001) and each layer has a two-fold screw axis parallel to the c axis (10). The (001) surface studied was freshly cleaved by using a sharp knife blade placed on a (210) face. A perfectly flat surface is necessary to achieve consistent dissolution features.

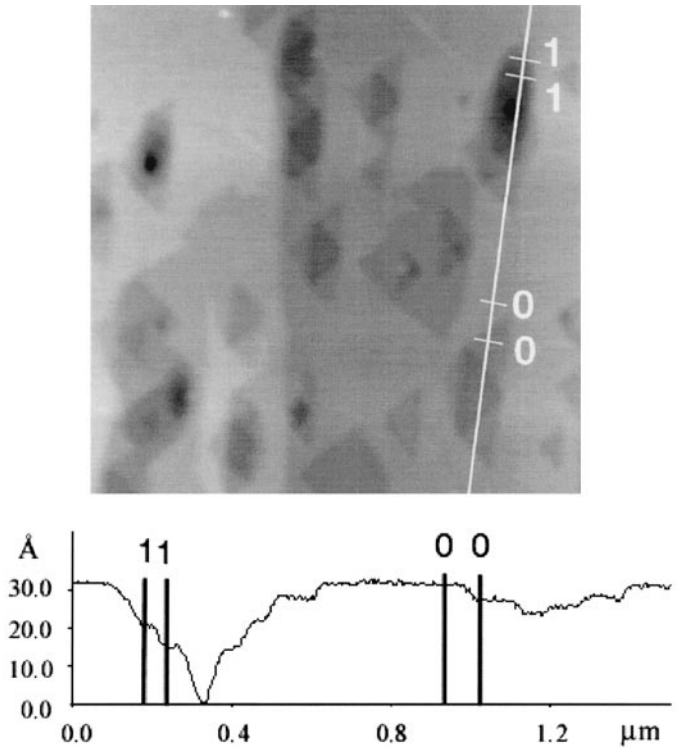

FIG. 4. Higher-magnification image of a region displayed in Fig. 3a and corresponding line profile along the *b* axis through two pits observed after immersion of the barite (001) surface in HCl for 15 min. The depths of the etch pits "0–0" and "1–1" are 3.61 and 7.02 Å, respectively. Image size: 1.5 μm × 1.5 μm. Depth scale from black to white: 5 nm.

A Park Scientific Instruments (PSI) Autoprobe CP was operated as an AFM in noncontact mode using triangularly shaped Si cantilevers with integrated triangular tips that were supplied by PSI. These cantilevers had oscillation frequencies of 220 kHz and spring constants of about 13 N/m. All images were collected in air under ambient conditions at room temperature. The sample was etched for a selected period (ranging from 5 to 60 min) at 20°C in aqueous solutions of 0.1 M HCl (EM Science), which were diluted from 36.5% (w/w) concentrated solutions with deionized water. After etching in solution, the crystal was taken out, rinsed well with deionized water, and dried prior to NC-AFM measurement.

RESULTS AND DISCUSSION

The barite sample used in this study contains about 10% Sr atoms as impurity (Sr/Ba = 0.0989). Since both strontium and barium sulfate are isostructural crystals, the presence of Sr^{2+} cations has little effect on the morphology of barium sulfate. Experimental studies of the effects of coprecipitated Sr^{2+} cations on $BaSO_4$ by Benton *et al.* (15) and molecular simulations of the overgrowth of $SrSO_4$ on $BaSO_4$ by Redfern and Parker (16) have reported that the morphology of the barium sulfate crystal is only slightly altered in the presence of strontium. Thus, we believe that the Sr^{2+} cations on $BaSO_4$ have little effect on the morphology of etch pits produced by HCl. However, Dove and Czank reported that $SrSO_4$ is about 50 times more soluble than $BaSO_4$ at pH 2 at 50°C (17). Consequently, we may observe larger and deeper etch pits if $SrSO_4$ is formed on the surfaces of $BaSO_4$.

A freshly cleaved barite (001) surface is characterized by flat terraces and steps of one or multiples of one unit cell height (i.e., c = 7.16 Å) (4, 6). A barite (001) surface that has been treated with HCl solution for 5 min is shown in Fig. 1. In the beginning of the dissolution process, shallow triangular etch pits (marked "1") with a depth of one-half unit cell (3.6 Å) formed and were distributed randomly over the surface. Subsequently, a second triangular feature with a depth of one unit cell and pointed oppositely to the first triangular pit developed inside the first pit (marked "2"). Deeper etch pits with depths of multiples of one-half unit cell (marked "3") were observed with increasing dissolution time. Figure 2 illustrates a line scan profile through three pits observed after 5 min at a higher magnification.

The changing orientations of the triangular features can be explained by the presence of the two-fold screw axis, which is oriented parallel to the *c* axis (4). The triangular etch pits have an obtuse angle of 97° ± 3°, indicating that the walls of the pits are bounded along [010], [120], and [1$\bar{2}$0] directions. In other words, these pits are bounded by {100} and {210} faces. The (210) face is one of the two lowest-energy surfaces in barite crystals under vacuum (16, 18, 19) as calculated by molecular simulations. Therefore, the geometry of these etch pits arises as a result of minimizing the surface energy.

Figure 3 shows a series of *ex situ* AFM images of barite (001) surfaces treated with 0.1 M HCl for 15, 25, 40, and 60 min. These images are representative of those obtained from different areas of the surface and reveal consistent and reproducible dissolution features for a particular dissolution time. After 15 min, deep and elongated etch pits (dark areas more than one unit cell in depth) were observed, as shown in Fig. 3a. These pits increased in size with increasing dissolution time as shown in Figs. 3b–3d. Etch pits were developed along the crystallographic *b* axis, and the growth rate of the etch pits along the *b* axis is much faster than that along the *a* and *c* axes. The deepest and largest etch pit shown in Fig. 3d has a depth:width:length ratio of approximately 1:146:485. These dimensions are indicative of an anisotropic growth of the etch pits. Most of the etch pits have a flat bottom, which is a consequence of the dissolution of several $BaSO_4$ layers (up to nine $BaSO_4$ layers). A line profile measurement of two pits observed after 15 min at higher magnification is shown in Fig. 4. The "stair step" features with heights of one-half or one unit cell suggest that the pits in the (001) surface were formed by a layer-by-layer dissolution process.

Comparisons with the etch pits induced by water at room temperature (20°C) (6) and high temperature (125°C) (8) reveal that the morphology of the HCl-etched pits is similar to the morphology of those in water. In water, the walls of the etch pits were also bounded along the ⟨120⟩ and ⟨010⟩ directions and the pits were composed of steps with depths that were multiples of one-half of the unit cell dimension, starting from a triangular pit geometry with a depth of one-half unit cell.

In HCl solution, pits are formed by approach of protons H^+ to the (001) surface, interaction with SO_4^{2-} anions, and subsequent removed of these from the lattice. The following mechanism can be used to explain barite dissolution:

$$H^+_{(aq)} + BaSO_{4(s)} \xrightarrow{k_1} Ba^{2+}_{(aq)} + HSO^-_{4(aq)}, \quad [1]$$

$$H^+_{(aq)} + HSO^-_{4(aq)} \underset{k_{-2}}{\overset{k_2}{\rightleftharpoons}} H_2SO_{4(aq)}. \quad [2]$$

Therefore, etch pits are formed that are one-half of the unit cell deep and are distributed randomly and mostly bounded by low-energy planes along the [120] and [1$\bar{2}$0] directions to form triangular features. Dissolution of barite surfaces in water and HCl are strongly controlled by the underlying $BaSO_4$ structure.

CONCLUSIONS

These experiments demonstrate that the surface structure of $BaSO_4$ has a significant influence on the geometry of etch pits created by dissolution in 0.1

M HCl. *Ex situ* observations by NC-AFM show that $BaSO_4$ (001) surfaces dissolve in HCl solutions by forming triangular etch pits that are one-half of the unit cell (3.6 Å) deep. These pits become gradually elongated and deeper in a layer-by-layer dissolution mechanism.

ACKNOWLEDGMENTS

T. F. Yen gratefully acknowledges financial support of this work by Chevron Petroleum Technology Company (CPTC) and donation of barite crystals from Barrick Meikle Mine. B. E. Koel acknowledges support of the Laboratory for Molecular Robotics by the Z. A. Kaprielian Technology Innovation Fund.

REFERENCES

1. Cowan, J. C., and Weintritt, D. J., "Water-Formed Scale Deposits." Gulf Publishing Co., Houston, 1976.
2. Högfeldt, E. "Stability Constants of Metal–Ion Complexes, Part A: Inorganic Ligands." Pergamon Press, Oxford, 1982.
3. Morris, R. L., and Paul, J. M., U.S. Patent 4,980,077 (Dec. 1990).
4. Putnis, A., Junya-Rosso, J. L., and Hochella, M. F., Jr., *Geochim. Cosmochim. Acta* **59,** 4623 (1995).
5. Bosbach, D., Hall, C., and Putnis, A., *Chem. Geol.* **151,** 143 (1998).
6. Wang, K. S., Resch, R., Dunn, K., Shuler, P., Tang, Y., Koel, B. E., and Yen, T. F., *Colloids Surf. A,* in press.
7. Wang, K. S., Resch, R., Dunn, K., Shuler, P., Tang, Y., Koel, B. E., and Yen, T. F., *Langmuir,* in press.
8. Higgins, S. R., Jordan, G., and Eggleston, C. M., *Langmuir* **14,** 4967 (1998).
9. Pina, C. M., Bosbach, D., Prieto, M., and Putnis, A., *J. Cryst. Growth* **187,** 119 (1998).
10. Pina, C. M., Becker, U., Risthaus, P., Bosbach, D., and Putnis, A., *Nature* **395,** 483 (1998).
11. Schmitz, I., Schreiner, M., Friedbacher, G., and Grasserbauer, M., *Anal. Chem.* **69,** 1012 (1997).
12. Itoh, T., Ohashi, T., and Suga, T., *J. Vac. Sci. Technol. B* **14,** 1577 (1996).
13. Overney, R. M., Takano, H., Fujihira, M., Meyer, E., and Güntherodt, H.-J., *Thin Solid Films* **240,** 105 (1994).
14. Miyake, M., Minato, I., Morikawa, H., and Iwai, S.-I., *Am. Mineral.* **63,** 506 (1978).
15. Benton, W. J., Collins, I. R., Grimsey, I. M., Parkinson, G. M., and Rodger, S. A., *Faraday Discuss.* **95,** 281 (1993).
16. Redfern, S. E., and Parker, S. C., *J. Chem. Soc. Faraday Trans.* **94,** 1947 (1998).
17. Dove, P. M., and Czank, C. A., *Geochim. Cosomochim. Acta* **59,** 1907 (1995).
18. Allan, N. L., Rohl, A. L., Gay, D. H., Catlow, R. A., Davey, R. J., and Mackrodt, W. C., *Faraday Discuss.* **95,** 272 (1993).
19. Blanco, M., Tang, Y., Shuler, P., and Goddard, W. A., III, *Mol. Eng.* **7,** 491 (1997).

Kang-Shi Wang

Department of Civil and Environmental Engineering
University of Southern California
Los Angeles, California 90089

Roland Resch
Bruce E. Koel

Department of Chemistry
University of Southern California
Los Angeles, California 90089

Patrick J. Shuler
Yongchun Tang
Huey-jyh Chen

Chevron Petroleum Technology Company
La Habra, California 90631

Teh Fu Yen[1]

Department of Civil and Environmental Engineering
University of Southern California
Los Angeles, California 90089

Received May 19, 1999; accepted July 30, 1999

[1] To whom correspondence should be addressed at Department of Civil and Environmental Engineering, University of Southern California, KAP Building 224A, Los Angeles, CA 90089–2531. Fax: (213) 744–1426. E-mail: tfyen@mizar.usc.edu.